4892 J. Med. Chem. 2009, 52, 4892–4902
DOI: 10.1021/jm900490a

Journal of Medicinal Chemistry Article

Design, Synthesis, and X-ray Crystal Structure of Classical and Nonclassical 2-Amino-4-oxo-5-substituted-6-ethylthieno[2,3-*d*]pyrimidines as Dual Thymidylate Synthase and Dihydrofolate Reductase Inhibitors and as Potential Antitumor Agents

Aleem Gangjee,*[,†] Wei Li,[†] Roy L. Kisliuk,[‡] Vivian Cody,[§] Jim Pace,[§] Jennifer Piraino,[§] and Jennifer Makin[§]

[†]*Division of Medicinal Chemistry, Graduate School of Pharmaceutical Sciences, Duquesne University, 600 Forbes Avenue, Pittsburgh, Pennsylvania 15282,* [‡]*Department of Biochemistry, School of Medicine, Tufts University, Boston, Massachusetts 02111, and* [§]*Hauptman-Woodward Medical Research Institute, Inc., 700 Ellicott Street, Buffalo, New York 14203*

Received April 17, 2009

N-{4-[(2-Amino-6-ethyl-4-oxo-3,4-dihydrothieno[2,3-*d*]pyrimidin-5-yl)thio]benzoyl}-L-glutamic acid **2** and 13 nonclassical analogues **2a**−**2m** were synthesized as potential dual thymidylate synthase (TS) and dihydrofolate reductase (DHFR) inhibitors and as antitumor agents. The key intermediate in the synthesis was 2-amino-6-ethyl-5-iodothieno[2,3-*d*]pyrimidin-4(3*H*)-one, **7**, to which various arylthiols were attached at the 5-position. Coupling **8** with L-glutamic acid diethyl ester and saponification afforded **2**. X-ray crystal structures of **2** and **1** (the 6-methyl analogue of **2**), DHFR, and NADPH showed for the first time that the thieno[2,3-*d*]pyrimidine ring binds in a "folate" mode. Compound **2** was an excellent dual inhibitor of human TS (IC_{50} = 54 nM) and human DHFR (IC_{50} = 19 nM) and afforded nanomolar GI_{50} values against tumor cells in culture. The 6-ethyl substitution in **2** increases both the potency (by 2−3 orders of magnitude) as well as the spectrum of tumor inhibition in vitro compared to the 6-methyl analogue **1**. Some of the nonclassical analogues were potent and selective inhibitors of DHFR from *Toxoplasma gondii*.

Introduction

Folate metabolism has long been recognized as an important and attractive target for chemotherapy because of its crucial role in the biosynthesis of nucleic acid precursors.[1,2] Inhibitors of folate-dependent enzymes have found clinical utility as antitumor, antimicrobial, and antiprotozoal agents[2−5] (Figure 1). Thymidylate synthase (TS[a]), which catalyzes the reductive methylation of deoxyuridylate (dUMP) to thymidylate (dTMP), has been of particular interest.[6,7] This reaction affords 7,8-dihydrofolate (7,8-DHF), which is reduced by dihydrofolate reductase (DHFR) to tetrahydrofolate (THF).[3,5−7] Thus, TS and DHFR are crucial for the synthesis of dTMP in dividing cells. Several TS and DHFR inhibitors, as separate entities, have found clinical utility as antitumor agents.[8−12] Usually a 2,4-diamino-substituted pyrimidine ring is considered important for potent DHFR inhibitory activity, while a 2-amino-4-oxopyrimidine or 2-methyl-4-oxopyrimidine ring is considered important for potent TS inhibitory activity.[3,7,8] Examples of clinically used TS and DHFR inhibitors are raltitrexed,[12] pemetrexed,[11] and methotrexate[13] (MTX), illustrated in Figure 1. Raltitrexed is a quinazoline analogue that is transported into cells via the reduced folate carrier (RFC) and undergoes rapid polyglutamylation by the enzyme folylpolyglutamate synthetase (FPGS).[14,15] Raltitrexed is approved as a first-line agent for advanced colorectal cancer in several European countries, Australia, Canada, and Japan. In pemetrexed a pyrrole ring replaces the pyrazine of folic acid and a methylene group replaces the N10-nitrogen in the bridge.[11] Pemetrexed contains a 6−5 fused pyrrolo[2,3-*d*]pyrimidine scaffold and is designated a multitargeted antifolate (MTA). Pemetrexed and its polyglutamylated metabolites are reported to be inhibitors of several important folate-dependent enzymes including TS, DHFR, glycinamide ribonucleotide formyltransferase (GARFT), and aminoimidazole carboxamide ribonucleotide formyltransferase (AICARFT).[11,16,17]

As part of a continuing effort to develop novel classical antifolates as antitumor agents, Gangjee et al.[18] reported the synthesis of *N*-{4-[(2-amino-6-methyl-4-oxo-3,4-dihydrothieno[2,3-*d*]pyrimidin-5-yl)sulfanyl]benzoyl}-L-glutamic acid **1** (Figure 2) as a potent dual inhibitor of TS and DHFR with IC_{50} values in the 10^{-8} M range. Compound **1** also demonstrated moderate inhibitory activity against the growth of several human tumor cell lines in the National Cancer Institute (NCI)[19] preclinical in vitro screen, with GI_{50} values of 10^{-5}−10^{-6} M or lower. The dual TS/DHFR inhibitory potency and tumor cell inhibitory activities of **1** were, in part, attributed to its C6-methyl group. Molecular modeling using SYBYL 8.0[20] indicated that compound **1** could bind to human DHFR in the "flipped" mode compared to folic acid, in which the sulfur atom of thieno ring is superimposed onto the 4-oxo moiety of folate. Additionally, molecular modeling of **1** in human TS suggested that homologation of the C6-methyl

*To whom correspondence should be addressed. Phone: 412-396-6070. Fax: 412-396-5593. E-mail: gangjee@duq.edu.

[a] Abbreviations: TS, thymidylate synthase; dUMP, deoxyuridylate; dTMP, deoxythymidylate; 7,8-DHF, 7,8-dihydrofolate; DHFR, dihydrofolate reductase; MTX, methotrexate; RFC, reduced folate carrier; FPGS, folylpolyglutamate synthetase; GARFT, glycinamide ribonucleotide formyltransferase; AICARFT, aminoimidazole carboxamide ribonucleotide formyltransferase; AIDS, acquired immunodeficiency syndrome; *P. carinii, Pneumocystis carinii*; *T. gondii, Toxoplasma gondii*; *E. coli, Escherichia coli*; PTX, piritrexim; NCI, National Cancer Institute.

 Published on Web 07/16/2009

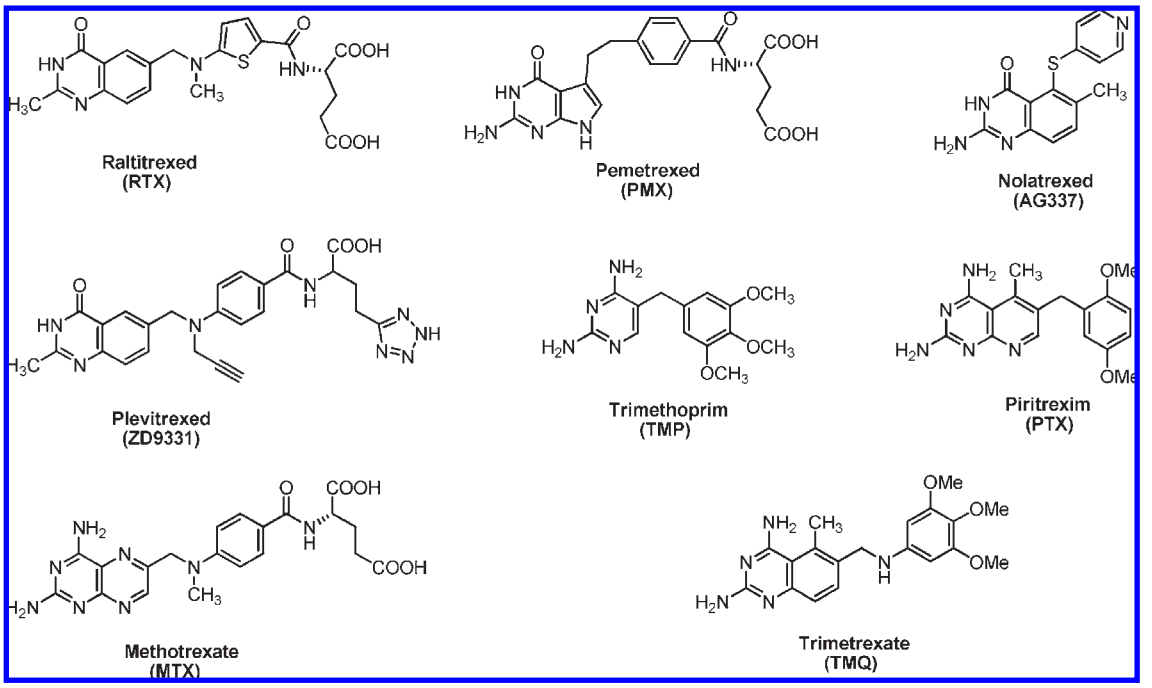

Figure 1. Representative antifolates.

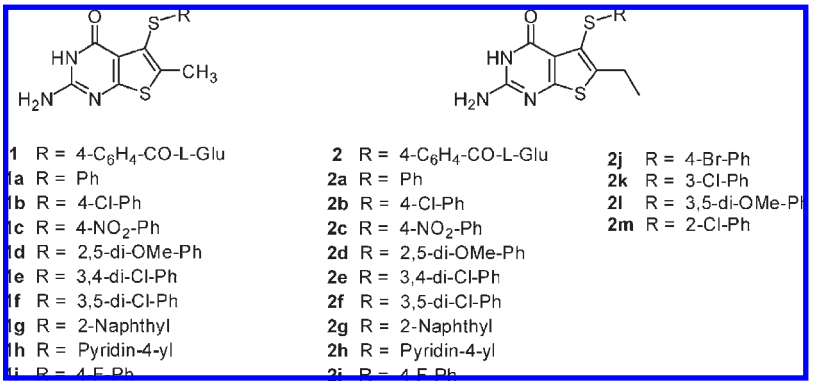

Figure 2. 6-Methyl and target 6-ethyl-2-amino-4-oxo-5-substituted thieno[2,3-*d*]pyrimidines.

to an ethyl could further enhance the hydrophobic interaction with Trp109 and perhaps the antitumor activity as well.

A disadvantage of classical antifolates as antitumor agents is that they require an active transport mechanism to enter cells, which, when impaired, causes tumor resistance.[21,22] In addition, cells that lack these transport mechanisms, including many bacterial and protozoan cells, are not susceptible to the action of classical antifolates.[23−26] In an attempt to overcome these potential drawbacks, nonclassical lipophilic antifolates have been developed as antitumor agents that do not require the folate transport system(s) but enter cells via diffusion. These lipophilic nonclassical antifolates such as nolatrexed (Figure 1) lack the polar glutamate moiety and hence do not depend on FPGS for their inhibitory activity.[27,28] In addition, nonclassical antifolates do not require the reduced folate carrier (RFC) system for active uptake into the cell, since they are lipophilic and are passively transported into cells.

An additional aspect of our interest in nonclassical dual TS-DHFR inhibitors lies in the treatment of opportunistic infections in immunocompromised patients such as those with acquired immunodeficiency syndrome (AIDS).[29,30] The principal cause of death in patients with AIDS is opportunistic infections caused by *Pneumocystis carinii* (*P. carinii*)[31] and *Toxoplasma gondii* (*T. gondii*).[32] Current therapy includes the use of selective but weak inhibitors of protozoal DHFR such as trimethoprim (TMP) (Figure 1), in combination with sulfonamides to enhance potency. Toxicity of the sulfa drug component of these combinations is often a serious problem.[32] The potent but toxic nonclassical antifolates trimetrexate (TMQ) and piritrexim (PTX) (Figure 1), coadministered with leucovorin for host rescue, are also used. Serious toxicities associated with the use of TMQ and PTX often force the cessation of treatment. Thus, it is of considerable interest to incorporate selectivity and potency into a single nonclassical antifolate that can be used alone to treat these infections.

Gangjee et al.[18] recently described the design and synthesis of several nonclassical 2-amino-4-oxo-5-arylthio-substituted-6-methylthieno[2,3-*d*]pyrimidines **1a**−**1i** (Figure 2) as dual TS/DHFR inhibitors. All of the nonclassical analogues were reasonably potent inhibitors of human TS with IC_{50} values ranging from 0.11 to 4.6 μM. The electronic nature of the substitutent on the side chain phenyl was an important factor in determining inhibitory potency. Analogues with electron

Scheme 1[a]

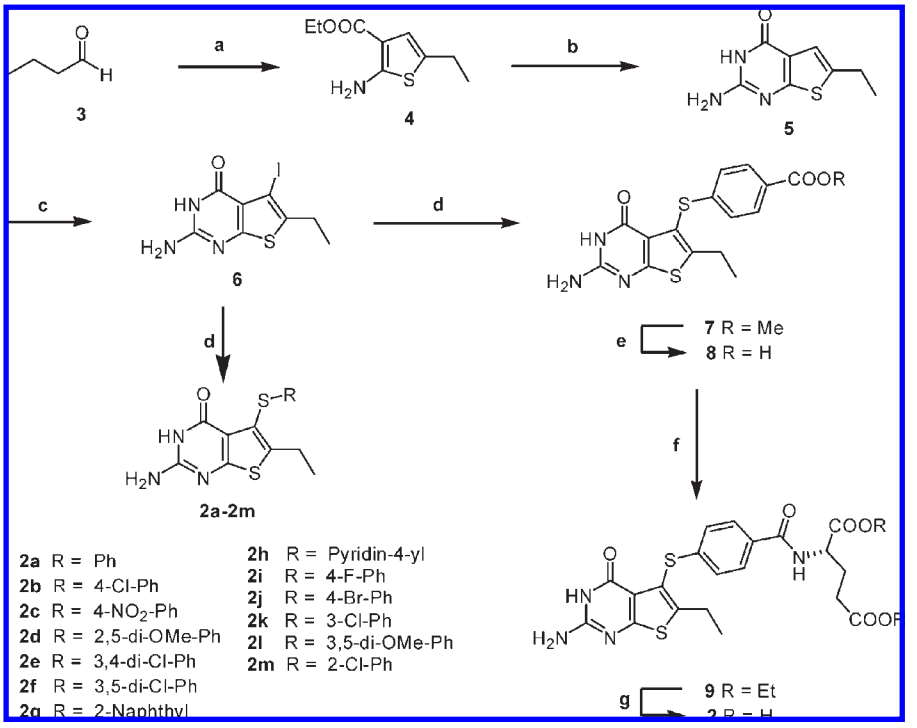

[a] Reagents: (a) ethyl cyanoacetate, Et_3N, sulfur, DMF, 55 °C, 3 h; (b) carbamimidic chloride hydrochloride, $DMSO_2$; 120 °C, 1 h; (c) (1) $Hg(AcO)_2$, AcOH, 100 °C, 3 h; (2) I_2, CH_2Cl_2, room temp, 5 h; (d) thiols, $Pd_2(dba)_3$, Xantphos, *i*-Pr_2NEt, DMF, microwave, 190 °C, 30 min; (e) 1 N NaOH, MeOH; (f) L-glutamate hydrochloride, 2-chloro-4,6-dimethoxy-1,3,5-triazine, *N*-methylmorpholine, DMF, room temp, 5 h; (g) 1 N NaOH, EtOH.

withdrawing substitutions on the phenyl ring were more potent than analogues with electron donating substitutions or the unsubstituted phenyl. Structure−activity relationship (SAR) studies demonstrated that analogues with electron withdrawing groups at the 3- and/or 4-position of the phenyl side chain provided optimum inhibitory potency against human TS. Nonclassical analogues such as **1b** ($IC_{50} = 0.26\ \mu M$), **1c** ($IC_{50} = 0.11\ \mu M$), **1e** ($IC_{50} = 0.11\ \mu M$), **1g** ($IC_{50} = 0.12\ \mu M$), or **1h** ($IC_{50} = 0.28\ \mu M$) were much more potent than the clinically used raltiterxed and pemetrexed against human TS; thus, nonclassical analogues **2a**−**2m** containing similar phenyl substituents were also synthesized. Interestingly, all the nonclassical compounds **1a**−**1i**[18]were potent inhibitors of *T. gondii* DHFR with IC_{50} values ranging from 0.028 to 0.12 μM. The IC_{50} values of compounds **1b**−**1i** against *T. gondii* DHFR were similar in potency to MTX and were about 243-fold more potent than the clinically used TMP. In addition, all the nonclassical compounds showed good to excellent selectivity against *T. gondii* DHFR compared to human DHFR. Analogue **1c** ($IC_{50} = 0.56\ \mu M$) was the most potent compound in this series against human DHFR, and it was 28-fold less potent against human DHFR than MTX but was more than 12-fold more potent than pemetrexed. Compound **1d** with a 2,5-dimethoxy substitution on the phenyl ring was marginally active against human DHFR ($IC_{50} = 22\ \mu M$) but very potent against *T. gondii* DHFR ($IC_{50} = 56$ nM), exhibiting 393-fold selectivity compared to human DHFR. As indicated above, molecular modeling (SYBYL 8.0) suggested that an extension of the 6-methyl group to an ethyl group might enhance the potency and selectivity against pathogenic TS and DHFR. To determine the effect of 6-ethyl homologation on human TS and DHFR inhibitory activity in the classical and nonclassical analogues, compounds **2**−**2m** (Figure 2) were synthesized. The synthesis and biological activities of analogues **2**−**2m** are the subject of this report.

Chemistry

The synthetic strategy for target compounds **2**−**2m** is shown in Scheme 1. The key intermediate in the synthesis was 2-amino-6-ethyl-5-iodothieno[2,3-*d*]pyrimidin-4(3*H*)-one, **6** (Scheme 1), which could undergo microwave assisted palladium catalyzed coupling reactions with appropriate arylthiols to afford target compounds **2a**−**2m** and intermediate **7** for the synthesis of classical analogue **2**.

The required intermediate ethyl 2-amino-5-ethylthiophene-3-carboxylate **4** was synthesized from commercially available butyraldehyde **3** with ethylcyanoacetate, sulfur, and triethylamine via reported methods of Gewald.[33] With compound **4** in hand, we turned our attention to its conversion to the 2-amino-6-ethylthieno[2,3-*d*]pyrimidin-4-(3*H*)-one, **5**. A literature search revealed that the synthesis of compound **5** was not reported. Gangjee et al.[34] had previously reported that chloroformamidine hydrochloride on cyclization with ethyl 2-amino-5-methylthiophene-3-carboxylate gave 2-amino-6-methylthieno[2,3-*d*]pyrimidin-4(3*H*)-one in reasonably good yield. Thus, heating a mixture of **4** and chloroformamidine hydrochloride in $DMSO_2$ under N_2 for a period of 2 h at 120−125 °C gave **5** in good yields (86%) after column chromatography.

Recently, we reported a convenient C5-bromination for the 2-amino-4-oxo-6-methylthieno[2,3-*d*]pyrimidine template with Br_2 under microwave irradiation.[18] To our surprise, all efforts to perform this halogenation of **5** with Br_2 or NBS using a variety of reaction conditions of time and temperature variations proved fruitless. Thus, we had to consider an alternative halogenation method. A search of the literature revealed that

there was no synthetic or other report for **6**. However, Taylor et al.[35] had reported a mercuration methodology that could be adopted for the synthesis of the key intermediate 2-amino-6-ethyl-5-iodothieno[2,3-*d*]pyrimidin-4(3*H*)-one **6**. Extending this methodology to the synthesis of **6** required the 5-chloromercury derivative, which was obtained by mercuration of **5** with mercurate acetate in glacial acetic acid at 100 °C for 3 h, followed by treatment with NaCl solution. Without separation, this 5-chloromercury derivative was treated with iodine in CH_2Cl_2 at room temperature for 5 h to afford **6** in 42% yield (over two steps). With the key intermediate **6** in hand, attention was turned to its conversion to the target compounds **2a**−**2m** and intermediate **7** (Scheme 1). Palladium-catalyzed cross-coupling reactions[36] to form carbon−sulfur bonds with aryl bromides and arylthiols appeared attractive for the synthesis of the target compounds **2a**−**2m** and intermediate **7**. Initial attempts to react the iodo derivative **6** with corresponding arylthiols catalyzed by $Pd_2(dba)_3$ with variations of time (up to 8 h) and temperature (up to reflux) were unsuccessful.

Failure of the above attempts led us to explore an alternative strategy to perform this palladium-catalyzed cross-coupling reaction. Microwave irradiation has been widely applied in organic synthesis, resulting in faster and cleaner reactions that sometimes exhibit different reactivities due to specific microwave absorption. It was therefore of interest to attempt this cross-coupling reaction under microwave irradiation. Thus, heating a mixture of **6**, the appropriate arylthiols, and *i*-Pr_2NEt in DMF in the presence of $Pd_2(dba)_3$ and Xantphos under microwave irradiation at 190 °C for 1 h afforded the corresponding target compounds **2a**−**2m** in yields of 67−87%.

For the synthesis of the classical compound **2**, the required intermediate, methyl 4-[(2-amino-6-ethyl-4-oxo-3,4-dihydrothieno[2,3-*d*]pyrimidin-5-yl)thio]benzoate, **7** (Scheme 1), was prepared using the same synthetic strategy as shown for **2a**−**2m**. Methyl 4-mercaptobenzoate was used to afford **7** in a yield of 76%. Ester hydrolysis of **7** with 1 N NaOH at room temperature for 18 h afforded the corresponding free acid **8** in 96% yield. Coupling of the acid **8** (Scheme 1) with L-glutamic acid diethyl ester hydrochloride and 2-chloro-4,6-dimethoxy-l,3,5-triazine as the activating agent followed by column chromatographic purification afforded **9** in 70% yield. The ^{1}H NMR of **9** revealed the newly formed peptide NH proton at 8.61 ppm as a doublet, which exchanged on addition of D_2O. Compound **9** was characterized on the basis of NMR and MS. Hydrolysis of **9** with aqueous NaOH at room temperature, followed by acidification with 3 N HCl under ice cold conditions, afforded target compound **2** in 94% yield.

X-ray Crystal Structure

The X-ray crystal structures of the ternary complex of **2**, NADPH, and the human DHFR double mutants (Q35K/N64F and Q35S/N64S) were determined, as well as complexes of **1** with the Q35K single mutant protein and wild type human DHFR. All DHFR ternary complex structures were refined to 1.3−1.5 Å resolution. These results show, for the first time, that the thieno[2,3-*d*]pyrimidine antifolates **1** and **2** bind in a folate orientation such that the thienosulfur occupies the N8 position observed in the binding of folic acid. Careful analysis of the difference electron density maps (Figure 3) was carried out to validate the binding orientation of **1** and **2**. The difference electron density for all structures reveals that the thieno ring of **1** and **2** bind in the folate orientation.

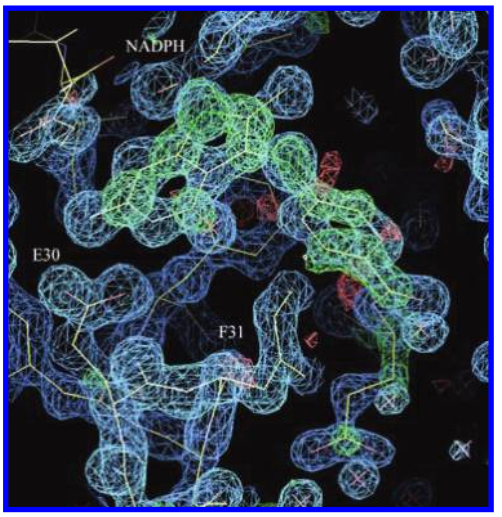

Figure 3. Difference electron density map ($2F_o-F_c$, 1σ, blue; F_o-F_c, 3σ, green) for the ternary complex of NADPH and **1** in human DHFR.

In these structures, the thieno ring has no hydrogen donor function. Nevertheless, the S7 of the thieno[2,3-*d*]pyrimidine ring makes intermolecular contacts with the carbonyl of Ile7 (3.6 Å), Val115 (3.9 Å), the hydroxyl of Tyr121 (3.8 Å), and the carbonyl of the nicotinamide ring (3.4 Å) (Figure 4). These values are longer than those observed for the 2,4-diaminopyrrolo[2,3-*d*]pyrimidine and furo[2,3-*d*]pyrimidine structures that showed a flipped orientation.[29,37,38] Although molecular modeling studies carried out previously[18] predicted that both a flipped and folate binding orientation was possible for 2-amino-4-oxo-6-methylthieno[2,3-*d*]pyrimidine, the structural data for four examples of **1** and **2** bound to mutant human DHFR all show binding in the folate orientation (Figure 5).

Biological Evaluation and Discussion

The classical analogue **2** and the nonclassical analogues **2a**−**2m** were evaluated as inhibitors of human, *Escherichia coli* (*E. coli*), and *T. gondii* DHFR[39] and TS.[40] The inhibitory potencies (IC_{50}) are listed in Table 1 and compared with those of pemetrexed, PDDF, MTX, and trimethoprim and the previously reported values for **1**.

The classical analogue **2** (Table 1) was an excellent dual inhibitor of human TS (IC_{50} = 54 nM) and human DHFR (IC_{50} = 19 nM). Against human TS, **2** was similar in potency to the previously reported compound **1** and about 2-fold more potent than PDDF and a remarkable 238-fold more potent than the clinically used pemetrexed.

Against human DHFR (Table 1) **2** was similar in potency to **1** and the clinically used MTX (Table 1) and was 330-fold more potent than pemetrexed. Interestingly, compound **2** was 9-fold more potent against *T. gondii* DHFR than human DHFR, indicating a significant species difference. Compound **2** was somewhat more potent than **1** as an inhibitor of human DHFR. This increase in activity against human DHFR of **2** over **1** may be attributed to increased hydrophobic interaction of the 6-ethyl moiety of **2** and Val115 in human DHFR as predicted from molecular modeling and confirmed by the X-ray crystal structure (Figure 6). The biological data (IC_{50}) of compounds **1** and **2** indicate that the methyl and ethyl groups at the C6-position, respectively, are both conducive for potent human TS and DHFR inhibition.

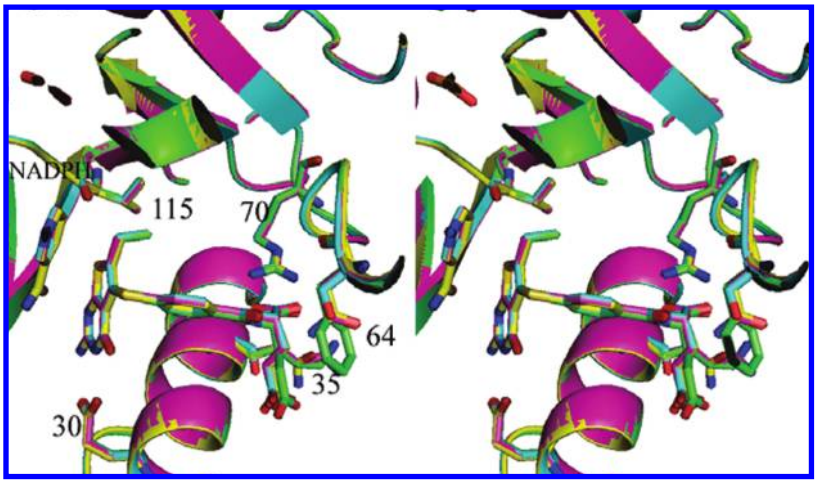

Figure 4. Stereoview of superposition of active site for human DHFR-Q35K/N64F double mutant ternary complex with the inhibitor **2** and NADPH (green), human DHFR-Q35S/N64S double mutant ternary complex with the inhibitor **2** and NADPH (cyan), human DHFR-Q35K single mutant ternary complex with **1** (violet), and human DHFR ternary complex with **1** (yellow). The figure was prepared with PyMol.

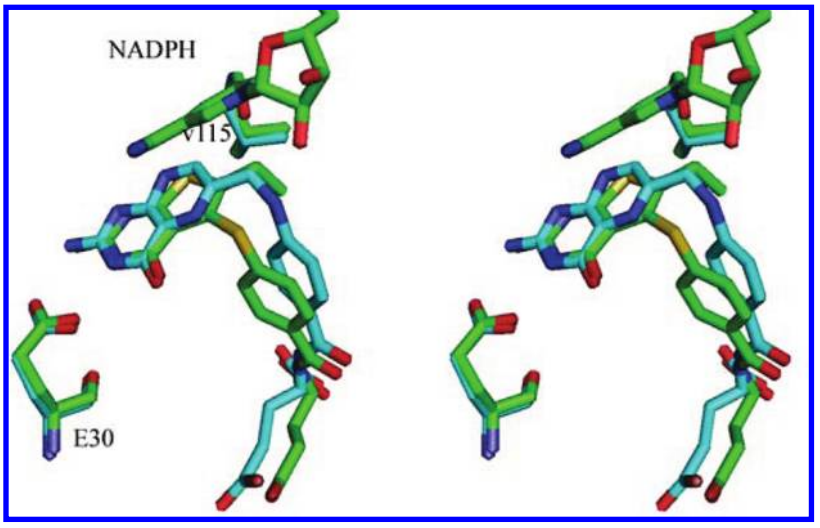

Figure 5. Stereoview of the superposition of folate (cyan) from hDHFR (PDB 1drf) on the structure of the hDHFR NADPH double mutant protein Q35K/N64F with **2** (green).

The nonclassical analogues **2a**−**2m** were also evaluated as inhibitors of TS and DHFR (Table 1). In the human TS assay, all of the nonclassical analogues were reasonably potent inhibitors with IC_{50} values ranging from 0.22 to 5.6 μM. The electronic nature of the substitutent on the side chain phenyl was an important factor in determining inhibitory potency. Analogues with electron withdrawing substitutions on the phenyl ring were more potent than analogues with electron donating substitutions or the unsubstituted phenyl. Electron withdrawing 4-nitro, 3,4-dichloro, 3-chloro, and 4-bromo substituents in analogues **2c**, **2e**, **2k** and **2j**, respectively, showed the most potent inhibition against isolated human TS. In addition, bulky substituents such as the 2-naphthyl (**2g**) showed marginal activity against human TS. These data are consistent with SAR studies previously reported for the C6-methyl analogues.[18] The nonclassical analogues **1b**, **1c**, **1e**, **1g**, and **1h** of the 6-methyl series were potent human TS inhibitors.[18] The corresponding 6-ethyl analogues **2b**, **2c**, **2e**, **2g**, and **2h** of this study were similar in potency except for **2g**, which was about 20-fold less potent than **1g**. This difference in potency may reflect a steric intolerance of the larger 6-ethyl moiety with an adjacent naphthyl ring in **2g**. Similar to the classical analogue **2**, all of the nonclassical analogues were also more potent than pemetrexed as inhibitors of human TS. This result indicates that homologation of a 6-methyl to a 6-ethyl in thieno[2,3-*d*]pyrimidines maintains potent human TS inhibitory activity.

In the DHFR assay, the nonclassical analogues **2a**−**2m** were also evaluated as inhibitors of human, *E. coli*, and *T. gondii* DHFR. Against human DHFR, in general **2a**−**2m** were moderately potent inhibitors with IC_{50} values ranging from 0.26 to 2.2 μM and were more potent than the corresponding 6-methyl analogues.[18] The most potent nonclassical analogues contained electron withdrawing groups such as 4-nitrophenyl **2c** (IC_{50} = 0.26 μM) and 4-bromophenyl **2j** (IC_{50} = 0.26 μM) in the 6-ethyl (**2a**−**2m**) series. Other substitutions such as an unsubstituted phenyl **2a** (IC_{50} = 2.6 μM) and unsubstituted 2-naphthyl **2g** (IC_{50} = 2.2 μM) cause a 10-fold drop in activity. In addition, compound **2c** was the most potent compound in the nonclassical series, also demonstrating potent dual inhibitory activities against human TS (IC_{50} = 0.22 μM) and human DHFR (IC_{50} = 0.26 μM). The SAR among these analogues (**2a**−**2m**) suggests that potency

Table 1. Inhibitory Concentrations (IC_{50} in μM) against TS and DHFR[a]

	TS (μM)			DHFR (μM)			
compd	human[b]	*E. coli*[b]	*T. gondii*[c]	human[d]	*E. coli*[e]	*T. gondii*[c]	rh/tg[f]
1[g]	0.04	0.04	0.036	0.02	0.2	0.008	2.5
2	0.054	0.018	0.09	0.019	1.0	0.0021	9
2a	5.6	28	8.4	2.6	>33 (10)	0.033	79
2b	0.75	2.5	2.2	0.3	42	0.009	33
2c	0.22	1.7	1.0	0.26	39	0.0087	30
2d	4.6	>23 (11)	>23 (29)	0.84	>28 (0)	0.014	60
2e	0.23	2.3	1.0	0.29	22	0.0081	36
2f	0.69	1.2	1.6	0.28	>2.8 (0)	0.014	20
2g	2.3	1.4	1.1	2.2	28	0.0084	262
2h	0.28	2.0	1.7	0.35	>33 (17)	0.017	21
2i	1.3	2.9	2.6	0.62	>31 (15)	0.025	25
2j	0.39	2.2	2.2	0.26	29	0.013	20
2k	0.38	2.3	1.8	0.3	>3.0 (0)	0.012	25
2l	1.2	1.8	2.3	0.54	>27 (0)	0.024	23
2m	1.1	2.0	2.5	0.6	>33 (0)	0.027	22
pemetrexed[h]	9.5	76	2.8	6.6	230	0.43	15
PDDF[i]	0.085	0.019	0.43	1.9	23	0.22	8.6
MTX	nd	nd	nd	0.02	0.0088	0.033	0.6
trimethoprim	nd	nd	nd	>340 (22)	0.01	6.8	>50

[a] The percent inhibition was determined at a minimum of four inhibitor concentrations within 20% of the 50% point. The standard deviations for determination of 50% points were within ±10% of the value given. Numbers in parentheses indicate the % inhibition at the stated concentration. nd = not determined. [b] Kindly provided by Dr. Frank Maley, New York State Department of Health. [c] Kindly provided by Dr. Karen Anderson, Yale University, New Haven, CT. [d] Kindly provided by Dr. J. H. Freisheim, Medical College of Ohio, Toledo, OH. [e] Kindly provided by Dr. R. L. Blakley, St. Jude Children's Hospital, Memphis, TN. [f] rh/tg is selectivity ratio for *T. gondii* DHFR and is the IC_{50} against rhDHFR/IC_{50} against *T. gondii* DHFR. [g] Data derived from ref 18. [h] Kindly provided by Dr. Chuan Shih, Eli Lilly and Co. [i] Kindly provided by Dr. M. G. Nair, University of South Alabama.

for human DHFR is independent of the electronic nature of the substituent but mono-para-electron-withdrawing substitution is most favorable for human DHFR inhibition. Against *T. gondii* DHFR, in general, the nonclassical analogues **2a**−**2m** were very potent inhibitors with IC_{50} values ranging from 0.27 to 0.0081 μM. The most potent single digit nanomolar nonclassical inhibitors contained electron withdrawing groups such as a 4-chlorophenyl **2b** (IC_{50} = 0.009 μM), 4-nitrophenyl **2c** (IC_{50} = 0.0087 μM), 3,4-dichlorophenyl **2e** (IC_{50} = 0.0081 μM), and 2-naphthyl **2g** (IC_{50} = 0.0084 μM). The IC_{50} values of compounds **2b**, **2c**, **2e**, and **2g** against *T. gondii* DHFR were a remarkable 4-fold more potent than MTX and were about 840-fold more potent than the clinically used trimethoprim (Table 1). To our knowledge these are some of the most potent nonclassical *T. gondii* DHFR inhibitors reported. Interestingly, a number of the nonclassical compounds in this series also showed good selectivity for *T. gondii* DHFR compared to human DHFR. Compound **2g** with a 2-naphthyl substitution was 262-fold more selective for T. gondii DHFR than human DHFR, which indicated a distinct species difference in DHFR from different sources. These results demonstrate that the nonclassical analogues **2a**−**2m** in the 6-ethyl series follow similar trends of dual inhibition against human TS and DHFR as the 6-methyl analogues.

Table 2. Cytotoxic Evaluation (GI_{50}, M) of Compounds **1** and **2** against Selected Tumor Cell Lines

cell line	GI_{50} of **1** (M)	GI_{50} of **2** (M)
	Leukemia	
CCRF-CEM	9.45×10^{-5}	8.53×10^{-7}
HL-60 (TB)		4.97×10^{-7}
MOLT-4	$> 1.00 \times 10^{-4}$	4.78×10^{-6}
	Non-Small-Cell Lung Cancer	
NCI-H460	4.12×10^{-5}	9.59×10^{-7}
NCI-H525	$> 1.00 \times 10^{-4}$	7.80×10^{-6}
NCI-H23	$> 1.00 \times 10^{-4}$	9.40×10^{-6}
	Colon Cancer	
HCC-2998	$> 1.00 \times 10^{-4}$	9.65×10^{-7}
HCT-116	$> 1.00 \times 10^{-4}$	2.84×10^{-7}
	Melanoma	
LOX IMVI	6.56×10^{-5}	9.09×10^{-8}
M14	$> 1.00 \times 10^{-4}$	4.32×10^{-6}
	Ovarian Cancer	
OVCAR-8	$> 1.00 \times 10^{-4}$	5.79×10^{-7}
	Renal Cancer	
786-0	$> 1.00 \times 10^{-4}$	8.17×10^{-7}
SN12C	$> 1.00 \times 10^{-4}$	3.31×10^{-6}

The classical analogue **2** was selected by the National Cancer Institute (NCI) for evaluation in its in vitro preclinical antitumor screening program. Approximately 60 human cancer cell lines of the full NCI panel are grouped into disease subpanels, including leukemia, non-small-cell lung, colon, central nervous system (CNS), melanoma, ovarian, renal, prostate, and breast tumors cell lines. The ability of compound **2** to inhibit the growth of tumor cell lines was measured as GI_{50} values, the concentration required to inhibit the growth of tumor cells in culture by 50% compared to a control. In 8 of the 60 cell lines, compound **2** showed GI_{50} values of $< 10^{-6}$ M (Table 2). It was also interesting to note that compound **2** was not a general cell poison but showed selectivity both within a type of tumor cell line and across different tumor cell lines with inhibitory values that in some instances differed by 1000-fold (data not shown). In addition, potency of tumor inhibition (GI_{50}) was significantly increased for **2** over **1** (Table 2) by 100- to 1000-fold, indicating that homologation of the 6-methyl to the 6-ethyl was instrumental in increasing the potency as well as the spectrum of tumor inhibition in culture (Table 2). Thus, the in vitro tumor cell inhibitory activity of **2** was much superior to that of **1**. Possible explanation for this increased in vivo activity could be the increased lipophilicity of **2** compared to **1**, which could facilitate passive diffusion and/or active transport of **2** into tumor cells. This is currently under investigation. Compound **2** is also currently under further evaluation by the NCI as an antitumor agent.

In summary, the 5-substituted 2-amino-4-oxo-6-ethylthieno[2,3-*d*]pyrimidine classical antifolate **2** and 13 nonclassical analogues **2a**−**2m** were designed and synthesized as potential dual TS-DHFR inhibitors. Compound **2** (TS IC_{50} = 54 nM; DHFR IC_{50} = 19 nM) maintained the potent human TS and DHFR inhibitory activity of **1**. More importantly compound **2** significantly increased both the spectrum and the potency of the inhibition of the growth of tumor cells in culture compared with **1**. This increase was clearly not attributable to enzyme inhibition difference because both **1** and **2** have about the same activity in isolated enzyme assays. Compound **2c** was the

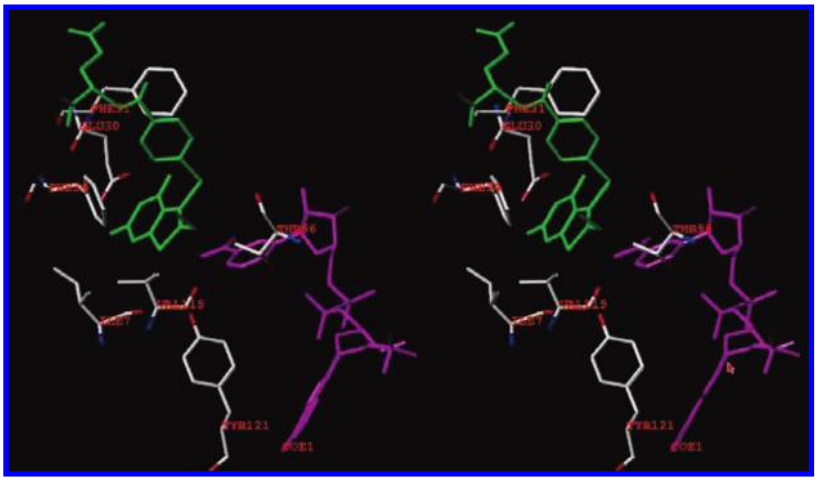

Figure 6. Stereoview of active site for human DHFR-Q35S/N64S double mutant ternary complex with the inhibitor **2** and NADPH. The figure was prepared with SYBY 8.0.

most potent compound in the nonclassical series, also demonstrating potent dual inhibitory activities against human TS (IC_{50} = 0.22 μM) and human DHFR (IC_{50} = 0.26 μM). In addition, excellent potency and high selectivity for *T. gondii* DHFR compared to human DHFR were observed for all the analogues. This study indicated that the 5-substituted 2-amino-4-oxo-6-ethylthieno[2,3-*d*]pyrimidine scaffold is the most conducive to dual human TS-DHFR inhibitory activity. The most remarkable finding was that elongation of the C6-methyl moiety of 2-amino-4-oxo-5-arylthio-substituted thieno[2,3-*d*]pyrimidine **1** to the 6-ethyl in **2** increases the inhibitory potency against the growth of several tumor cells in culture by 2−3 orders of magnitude and also increases the spectrum of tumor growth inhibition. These results are currently under investigation and may reflect transport and/or other differences between **1** and **2**.

Experimental Section

Analytical samples were dried in vacuo (0.2 mmHg) in a CHEM-DRY drying apparatus over P_2O_5 at 80 °C. Melting points were determined on a MEL-TEMP II melting point apparatus with a FLUKE 51 K/J electronic thermometer and are uncorrected. Nuclear magnetic resonance spectra for proton (^{1}H NMR) were recorded on a Bruker WH-400 (400 MHz) spectrometer. The chemical shift values are expressed in ppm (parts per million) relative to tetramethylsilane as an internal standard: s, singlet; d, doublet; t, triplet; q, quartet; m, multiplet; br, broad singlet. Mass spectra were recorded on a VG-7070 double-focusing mass spectrometer or in a LKB-9000 instrument in the electron ionization (EI) mode. Chemical names follow IUPAC nomenclature. Thin-layer chromatography (TLC) was performed on Whatman Sil G/UV254 silica gel plates with a fluorescent indicator, and the spots were visualized under 254 and 366 nm illumination. Proportions of solvents used for TLC are by volume. Column chromatography was performed on a 230−400 mesh silica gel (Fisher, Somerville, NJ) column. Elemental analyses were performed by Atlantic Microlab, Inc., Norcross, GA. Element compositions are within 0.4% of the calculated values. Fractional moles of water or organic solvents frequently found in some analytical samples of antifolates could not be prevented in spite of 24−48 h of drying in vacuo and were confirmed where possible by their presence in the ^{1}H NMR spectra. Microwave-assisted synthesis was performed utilizing an Emrys Liberator microwave synthesizer (Biotage) utilizing capped reaction vials. All microwave reactions were performed with temperature control. All solvents and chemicals were purchased from Aldrich Chemical Co. or Fisher Scientific and were used as received.

Ethyl 2-Amino-5-ethylthiophene-3-carboxylate (4). Et_3N (4.7 g, 0.05 mol) was added to a stirred suspension of ethyl cyanoacetate (9.74 g, 90 mmol) and sulfur (2.76 g, 90 mol) in 50 mL of DMF under a N_2 atmosphere. The resulting mixture was stirred at 55 °C (temperature of bath) for 1 h. Butyraldehyde **3** (6.5 g, 90 mmol) was then added into this suspension dropwise while maintaining the temperature at 55 °C. After addition, the mixture was allowed to cool to room temperature and stirred for 2 h. The mixture was transferred to a separating funnel containing ethyl acetate (80 mL) and H_2O (30 mL). The organic layer was separated, washed with brine (4 × 20 mL), and concentrated under reduced pressure to afford a yellow oil. The residue was loaded on a column packed with silica gel and eluted with 5% ethyl acetate in hexanes, and fractions containing the desired product (TLC) were pooled and evaporated to afford 8.9 g (56%) of **4** as a yellow solid: mp 70−72 °C; R_f = 0.45 (ethyl acetate/*n*-hexane, 1:3); ^{1}H NMR (DMSO-d_6) δ 1.08 (t, 3 H, J=7.2 Hz), 1.19 (t, 3 H, J=7.2 Hz), 2.48 (q, 2 H, J=7.2 Hz), 4.11 (q, 2 H, J = 7.2 Hz), 6.45 (s, 1H), 7.07 (s, 2 H).

2-Amino-6-ethylthieno[2,3-*d*]pyrimidin-4-(3*H*)-one (5). Ethyl 2-amino-5-ethylthiophene-3-carboxylate **4** (9.5 g, 47.8 mmol), carbamimidic chloride hydrochloride (5.5 g, 48.3 mmol), and 25 g of $DMSO_2$ was placed in a 250 mL flask. The reaction mixture was heated to 120−125 °C under N_2 for 2 h. Then H_2O (50 mL) was added to the reaction mixture right away to quench the reaction. The resulting solution was cooled in an ice bath, and the pH was adjusted to 8 with dropwise addition of concentrated NH_4OH with stirring. This suspension was left at 5 °C for 3 h and filtered. The residue was washed well with small amounts of acetone and water and purified by flash chromatography on silica gel (gradient of 2% MeOH/$CHCl_3$ to 5% MeOH/$CHCl_3$) to afford 8.1 g (86%) of **5** as a yellow solid: mp 126−128 °C; R_f = 0.63 (MeOH/$CHCl_3$, 1:10); ^{1}H NMR (DMSO-d_6) δ 1.20 (t, 3 H, J = 7.6 Hz), 2.71 (q, 2 H, J = 7.6 Hz), 6.45 (s, 2 H), 6.79 (s, 1 H), 10.82 (s, 1 H). Anal. ($C_8H_9N_3OS \cdot 0.09CH_3COCH_3$) C, H, N, S.

2-Amino-6-ethyl-5-iodothieno[2,3-*d*]pyrimidin-4(3*H*)-one (6). To a suspension of **5** (3.5 g, 17.9 mmol) in 50 mL of glacial acetic acid at room temperature was added mercuric acetate (8.5 g, 26.8 mmol). The resulting solution was stirred at 100 °C for 3 h, then poured into a saturated NaCl (50 mL), and stirred for 20 min. The solid was collected by filtration, washed with water (20 mL), hexane (20 mL), and dried to give a dark solid (5-chloromercury derivative), which was directly used for iodination reaction without further purification. This dark material was dissolved in CH_2Cl_2 (30 mL) containing I_2 (6.8 g, 26.8 mmol)

and stirred for 5 h at room temperature. The solvent was evaporated, and the residue was washed with 2 N NaS_2O_3 (35 mL) and dried in vacuo. The crude product was purified by column chromatography on silica gel with 3% MeOH/$CHCl_3$ as the eluent to afford 2.4 g (42%) of **6** as a white solid: mp 185−187 °C; R_f = 0.45 (MeOH/$CHCl_3$, 1:5); ^{1}H NMR (DMSO-d_6) δ 1.13 (t, 3 H, J = 7.6 Hz), 2.67 (q, 2 H, J = 7.6 Hz), 6.57 (s, 2 H), 10.93 (s, 1 H). Anal. ($C_8H_8IN_3OS \cdot 0.34CH_2Cl_2$) C, H, N, I, S.

Methyl 4-[(2-Amino-6-ethyl-4-oxo-3,4-dihydrothieno[2,3-*d*]-pyrimidin-5-yl)thio]benzoate (7). The microwave reaction vial was charged with **6** (1.05 g, 3.3 mmol), *i*-Pr_2NEt (1.2 mL, 6.6 mmol), and 15 mL dry DMF. The mixture was evacuated and backfilled with nitrogen (three cycles). Catalyst Pd_2dba_3 (76 mg, 0.08 mmol), Xantphos (94 mg, 0.16 mmol), and methyl 4-mercaptobenzoate (1.1 g, 6.6 mmol) were added, and then the reaction mixture was degassed twice. The reaction mixture was irradiated in a microwave apparatus at 190 °C, 1 h. After the reaction mixture was cooled to ambient temperature, the product was filtered, the filtrate was concentrated, and the crude mixture was purified by silica gel column chromatography using 2% MeOH in $CHCl_3$ as the eluent. Fractions containing the product (TLC) were combined and evaporated to afford 0.9 g (76%) of **7** as a white solid: R_f = 0.47 (MeOH/$CHCl_3$, 1:5); mp 156−158 °C; ^{1}H NMR (DMSO-d_6) δ 1.10 (t, 3 H, J = 7.2 Hz), 2.81 (q, 2 H, J = 7.2 Hz), 6.61 (s, 2 H), 7.05 (d, 2 H, J = 8.4 Hz), 7.77 (d, 2 H, J = 8.4 Hz), 10.79 (s, 1 H). HRMS (EI) calcd for $C_{16}H_{15}N_3O_3S_2$ m/z = 361.0554, found m/z = 361.0556.

2-Amino-6-ethyl-5-(phenylsulfanyl)thieno[2,3-*d*]pyrimidin-4(3*H*)-one (2a). Compound **2a** was synthesized as described for **7**: yield 87%; mp 215−220 °C; TLC R_f = 0.48 ($CHCl_3$/MeOH, 5:1); ^{1}H NMR (DMSO-d_6) δ 1.10 (t, 3 H, J = 7.6 Hz), 2.82 (q, 2 H, J = 7.6 Hz), 6.57 (s, 2 H), 6.97−7.24 (m, 5 H), 10.76 (s, 1 H). HRMS (EI) calcd for $C_{14}H_{13}N_3OS_2$ m/z = 303.0500, found m/z = 303.0503.

2-Amino-5-[(4-chlorophenyl)sulfanyl]-6-ethylthieno[2,3-*d*]pyrimidin-4(3*H*)-one (2b). Compound **2b** was synthesized as described for **7**: yield 81%; mp 174−175 °C; TLC R_f = 0.47 ($CHCl_3$/MeOH, 5:1); ^{1}H NMR (DMSO-d_6) δ 1.11 (t, 3 H, J = 7.6 Hz), 2.82 (q, 2 H, J = 7.6 Hz), 6.59 (s, 2 H), 6.98 (d, 2 H, J = 8.4 Hz), 7.27 (d, 2 H, J = 8.4 Hz), 10.76 (s, 1 H). HRMS (EI) calcd for $C_{14}H_{12}N_3OClS_2$ m/z = 337.0110, found m/z = 337.0093.

2-Amino-6-ethyl-5-[(4-nitrophenyl)sulfanyl]thieno[2,3-*d*]pyrimidin-4(3*H*)-one (2c). Compound **2c** was synthesized as described for **7**: yield 74%; mp 162−163 °C; TLC R_f = 0.48 ($CHCl_3$/MeOH, 5:1); ^{1}H NMR (DMSO-d_6) δ 1.12 (t, 3 H, J = 7.6 Hz), 2.82 (q, 2 H, J = 7.6 Hz), 6.64 (s, 2 H), 7.16 (d, 2 H, J = 9.2 Hz), 8.07 (d, 2 H, J = 9.2 Hz), 10.83 (s, 1 H). HRMS (EI) calcd for $C_{14}H_{13}N_4O_3S_2$ m/z = 349.0429, found m/z = 349.0403.

2-Amino-5-[(2,5-dimethoxyphenyl)sulfanyl]-6-ethylthieno[2,3-*d*]pyrimidin-4(3*H*)-one (2d). Compound **2d** was synthesized as described for **7**: yield 82%; mp 178−180 °C; TLC R_f = 0.50 ($CHCl_3$/MeOH, 5:1); ^{1}H NMR (DMSO-d_6) δ 1.08 (t, 3 H, J = 7.2 Hz), 2.77 (q, 2 H, J = 7.2 Hz), 3.52 (s, 3 H), 3.79 (s, 3 H), 5.92 (s, 2 H), 6.58−6.88 (m, 3 H), 10.78 (s, 1 H). HRMS (EI) calcd for $C_{16}H_{17}N_3O_3S_2$ m/z = 363.0711, found m/z = 363.0706.

2-Amino-5-[(3,4-dichlorophenyl)thio]-6-ethylthieno[2,3-*d*]pyrimidin-4(3*H*)-one (2e). Compound **2e** was synthesized as described for **7**: yield 72%; mp 154−116 °C; TLC R_f = 0.48 ($CHCl_3$/MeOH, 5:1); ^{1}H NMR (DMSO-d_6) δ 1.12 (t, 3 H, J = 7.6 Hz), 2.86 (q, 2 H, J = 7.6 Hz), 6.62 (s, 2 H), 6.90 (dd, 1 H, J = 2.4 Hz, J = 8.4 Hz), 7.3 (d, 2 H, J = 2.4 Hz), 7.46 (d, 1 H, J = 8.4 Hz), 10.80 (s, 1 H). HRMS (EI) calcd for $C_{14}H_{11}N_3OS_2Cl_2$ m/z = 370.9715, found m/z = 370.9720.

2-Amino-5-[(3,5-dichlorophenyl)sulfanyl]-6-ethylthieno[2,3-*d*]-pyrimidin-4(3*H*)-one (2f). Compound **2f** was synthesized as described for **7**: yield 74%; mp 176−178 °C; TLC R_f = 0.45 ($CHCl_3$/MeOH, 5:1); ^{1}H NMR (DMSO-d_6) δ 1.12 (t, 3 H, J = 7.6 Hz), 2.84 (q, 2 H, J = 7.6 Hz), 6.58 (s, 2 H), 6.98 (s, 1 H), 7.05 (s, 1 H), 7.20 (s, 1 H), 10.76 (s, 1 H). HRMS (EI) calcd for $C_{14}H_{11}N_3OS_2Cl_2$ m/z = 370.9708, found m/z = 370.9720.

2-Amino-6-ethyl-5-(2-naphthylthio)thieno[2,3-*d*]pyrimidin-4(3*H*)-one (2g). Compound **2g** was synthesized as described for **7**: yield 87%; mp 154−156 °C; TLC R_f = 0.51 ($CHCl_3$/MeOH, 5:1); ^{1}H NMR (DMSO-d_6) δ 1.12 (t, 3 H, J = 7.2 Hz), 2.86 (q, 2 H, J = 7.2 Hz), 6.59 (s, 2 H), 7.15−7.82 (m, 7 H), 10.74 (s, 1 H). HRMS (EI) calcd for $C_{18}H_{15}N_3OS_2$ m/z = 353.0656, found m/z = 353.0653.

2-Amino-6-ethyl-5-(pyridin-4-ylsulfanyl)thieno[2,3-*d*]pyrimidin-4(3*H*)-one (2h). Compound **2h** was synthesized as described for **7**: yield 67%; mp 185−186 °C; TLC R_f = 0.50 ($CHCl_3$/MeOH, 5:1); ^{1}H NMR (DMSO-d_6) δ 1.11 (t, 3 H, J = 7.2 Hz), 2.80 (q, 2 H, J = 7.2 Hz), 6.63 (s, 2 H), 6.92 (d, 2 H, J = 4.8 Hz), 8.28 (d, 2 H, J = 4.8 Hz), 10.83 (s, 1 H). HRMS (EI) calcd for $C_{13}H_{13}N_4OS_2$ m/z = 305.0531, found m/z = 305.0528.

2-Amino-6-ethyl-5-[(4-fluorophenyl)sulfanyl]thieno[2,3-d]pyrimidin-4(3*H*)-one (2i). Compound **2i** was synthesized as described for **7**: yield 75%; mp 194−196 °C; TLC R_f = 0.50 ($CHCl_3$/MeOH, 5:1); ^{1}H NMR (DMSO-d_6) δ 1.12 (t, 3 H, J = 7.2 Hz), 2.84 (q, 2 H, J = 7.2 Hz), 6.59 (s, 2 H), 7.07−7.09 (m, 4 H), 10.77 (s, 1 H). HRMS (EI) calcd for $C_{14}H_{12}N_3OFS_2$ m/z = 321.0405, found m/z = 321.0404.

2-Amino-5-[(4-bromophenyl)sulfanyl]-6-ethylthieno[2,3-*d*]pyrimidin-4(3*H*)-one (2j). Compound **2j** was synthesized as described for **7**: yield 74%; mp 186−187 °C; TLC R_f = 0.51 ($CHCl_3$/MeOH, 5:1); ^{1}H NMR (DMSO-d_6) δ 1.11 (t, 3 H, J = 7.2 Hz), 2.82 (q, 2 H, J = 7.2 Hz), 6.60 (s, 2 H), 6.92 (d, 2 H, J = 6.8 Hz), 7.39 (d, 2 H, J = 6.8 Hz), 10.76 (s, 1 H). HRMS (EI) calcd for $C_{14}H_{12}N_3OBrS_2$ m/z = 380.9611, found m/z = 380.9605.

2-Amino-5-[(3-chlorophenyl)sulfanyl]-6-ethylthieno[2,3-*d*]pyrimidin-4(3*H*)-one (2k). Compound **2k** was synthesized as described for **7**: yield 72%; mp 186−187 °C; TLC R_f = 0.53 ($CHCl_3$/MeOH, 5:1); ^{1}H NMR (DMSO-d_6) δ 1.14 (t, 3 H, J = 7.2 Hz), 2.87 (q, 2 H, J = 7.2 Hz), 6.62 (s, 2 H), 6.90 (m, 3 H), 7.24 (s, 1H), 10.80 (s, 1 H). HRMS (EI) calcd for $C_{14}H_{12}ClN_3OS_2$ m/z = 337.0119, found m/z = 337.0110.

2-Amino-5-[(3,5-dimethoxyphenyl)sulfanyl]-6-ethylthieno[2,3-*d*]pyrimidin-4(3*H*)-one (2l). Compound **2l** was synthesized as described for **7**: yield 83%; mp 151−154 °C; TLC R_f = 0.45 ($CHCl_3$/MeOH, 5:1); ^{1}H NMR (DMSO-d_6) δ 1.14 (t, 3 H, J = 7.6 Hz), 2.89 (q, 2 H, J = 7.6 Hz), 3.67 (s, 3 H), 6.55 (s, 2 H), 6.56 (dd, 1 H, J = 2.4 Hz, J = 8.4 Hz), 6.83 (d, 2 H, J = 2.4 Hz), 6.87 (d, 1 H, J = 8.4 Hz), 10.78 (s, 1 H). HRMS (EI) calcd for $C_{16}H_{17}N_3O_3S_2$ m/z = 363.0721, found m/z = 363.0711.

2-Amino-5-[(2-chlorophenyl)sulfanyl]-6-ethylthieno[2,3-*d*]pyrimidin-4(3*H*)-one (2m). Compound **2m** was synthesized as described for **7**: yield 72%; mp 221−224 °C; TLC R_f = 0.53 ($CHCl_3$/MeOH, 5:1); ^{1}H NMR (DMSO-d_6) δ 1.14 (t, 3 H, J = 7.2 Hz), 2.85 (q, 2 H, J = 7.2 Hz), 6.63 (s, 2 H), 6.90 (m, 4 H), 10.80 (s, 1 H). HRMS (EI) calcd for $C_{14}H_{12}ClN_3OS_2$ m/z = 337.0113, found m/z = 337.0110.

4-[(2-Amino-6-ethyl-4-oxo-3,4-dihydrothieno[2,3-*d*]pyrimidin-5-yl)thio]benzoic Acid (8). To a solution of **7** (0.72 g, 1.6 mmol) in MeOH (10 mL) was added 1 N NaOH (32 mL) and the reaction mixture stirred at room temperature for 18 h until TLC showed that the reaction was complete. The reaction mixture was evaporated to dryness under reduced pressure. The residue was diluted with H_2O (5 mL). The resulting solution was adjusted to pH 4 with 3 N aqueous HCl and then stored at 0 °C for 24 h. The precipitated solid was collected and dried in vacuo using P_2O_5 to afford 0.53 g (96%) of **8** as a white powder: mp 216−218 °C; R_f = 0.34 (MeOH/$CHCl_3$, 1:4); ^{1}H NMR (DMSO-d_6) δ 1.13 (t, 3 H, J = 7.6 Hz), 2.83 (q, 2 H, J = 7.6 Hz), 6.62 (s, 2 H), 7.03 (d, 2 H, J = 8.4 Hz), 7.76 (d, 2 H, J = 8.4 Hz), 10.79 (s, 1 H). Anal. ($C_{15}H_{13}N_3O_3S_2 \cdot 1.94CH_3COCH_3$) C, H, N, S.

Diethyl *N*-{4-[(2-Amino-6-ethyl-4-oxo-3,4-dihydrothieno[2,3-*d*]pyrimidin-5-yl)thio]benzoyl}-L-glutamate (9). To a suspension

Table 3. Data Collection and Refinement Statistics for Human DHFR-NADPH Ternary Complexes for **1** and **2**

parameter	Q35S/N64S NADPH-**2**	Q35K/N64F NADPH-**2**	wild type NADPH-**1**	Q35K NADPH-**1**
data collection				
PDB accession no.	3ghc	3ghv	3ghw	3gi2
space group	*H*3	*H*3	*H*3	*H*3
cell dimensions (Å)	84.36, 77.77	84.21, 78.03	84.56, 78.05	84.57, 77.94
beamline	SSRL 11-1	SSRL 11-1	SSRL 9-2	SSRL 9-2
resolution (Å)	1.01	1.20	1.20	1.50
wavelength (Å)	1.00	1.00	1.00	1.00
R_{sym} (%)[a,b]	0.050 (0.162)	0.058 (0.121)	0.036(2.3)	0.046 (0.29)
R_{merge}	0.045 (0.14)	0.044 (0.10)	0.114(4.2)	0.037 (0.25)
completeness (%)[a]	99.8 (95.3)	100.0 (99.8)	100.0 (94.0)	98.9 (98.9)
observed reflections	269 146	388 944	839 426	64 773
unique reflections	50 745	50 446	85 159	32 939
$I/\sigma(I)$	23.0 (10.3)	26.3 (11.2)	15.1 (0.3)	11.6 (2.5)
multiplicity[a]	5.3 (4.3)	5.3 (4.3)	9.9 (4.1)	2.0 (1.9)
refinement and model quality				
resolution range (Å)	26.0−1.30	53.3−1.30	22.59−1.24	42.30−1.53
no. of reflections	48 155	48 184	56 537	29 450
R-factor[c]	17.0	15.9	18.0	15.7
R_{free}-factor[d]	19.8	18.3	20.0	20.1
total protein atoms	1942	2030	1933	1939
total water atoms	354	384	347	358
average *B*-factor (Å^2)	13.8	14.0	18.2	18.3
rms deviation from ideal				
bond lengths (Å)	0.009	0.029	0.009	0.010
bond angles (deg)	1.858	1.943	1.76	1.73
Luzzati	0.131	0.127	0.144	0.143
Ramachandran plot				
most favored regions (%)	97.8	98.9	98.9	97.8
additional allowed regions (%)	2.2	1.1	1.1	2.2
generously allowed regions (%)	0.0	0.0	0.0	0.0
disallowed regions (%)	0.0	0.0	0.0	0.0

[a] The values in parentheses refer to data in the highest resolution shell. [b] $R_{sym} = \sum_h\sum_i|I_{h,i} - \langle I_h\rangle|/\sum_h\sum_i|I_{h,i}|$, where $\langle I_h\rangle$ is the mean intensity of a set of equivalent reflections. [c] *R*-factor $= \sum|F_{obs} - F_{calc}|/\sum F_{obs}$, where F_{obs} and F_{calc} are observed and calculated structure factor amplitudes. [d] R_{free}-factor was calculated for *R*-factor for a random 5% subset of all reflections.

of benzoic acid **8** (0.4 g, 1.1 mmol) in DMF (10 mL) at 25 °C was added *N*-methylmorpholine (0.12 mL, 1.21 mmol) followed by 2-chloro-4,6-dimethoxy-1,3,5-triazine (0.21 g, 1.1 mmol), and the resulting solution was stirred at 25 °C for 2 h. At this point, *N*-methylmorpholine (0.12 mL, 1.21 mmol) was added to this solution followed by L-glutamic acid diethyl ester hydrochloride (0.31 g, 1.32 mmol), and the resulting mixture was stirred at 25 °C for another 4 h until the starting material **8** disappeared (TLC). The reaction solution was evaporated in vacuo to dryness, and the residue was purified by column chromatography on silica gel with 5% MeOH in $CHCl_3$ as the eluent. Fractions containing the product (TLC) were combined and evaporated to afford 0.41 g (70%) of **9** as a white solid: mp 150−152 °C; R_f = 0.57 (MeOH/$CHCl_3$, 1:5); ^{1}H NMR (DMSO-d_6) δ 1.12−1.17 (m, 6 H), 1.14 (t, 3 H, J = 7.6 Hz), 1.93−2.10 (m, 2 H), 2.39 (m, 2 H), 2.86 (q, 2 H, J = 7.6 Hz), 4.05 (m, 4 H), 4.37 (m, 1 H), 6.61 (s, 1 H), 7.02 (d, 2 H, J = 8.4 Hz), 7.69 (d, 2 H, J = 8.4 Hz), 8.61 (d, 1 H, J = 7.6 Hz), 10.79 (br s, 1 H). Anal. ($C_{24}H_{28}N_4O_6S_2\cdot 0.59CH_3COCH_3$) C, H, N, S. HRMS (EI) calcd for $C_{24}H_{28}N_4O_6S_2$ m/z = 532.1450, found m/z = 532.1444.

***N*-{4-[(2-Amino-6-ethyl-4-oxo-3,4-dihydrothieno[2,3-*d*]pyrimidin-5-yl)thio]benzoyl}-L-glutamic Acid (2).** To a solution of **9** (0.35 g, 0.65 mmol) in ethanol (10 mL) was added 1 N NaOH (10 mL), and the mixture was stirred at room temperature for 24 h until the starting material **9** disappeared (TLC). The reaction mixture was evaporated to dryness under reduced pressure. The residue was dissolved in water (3 mL), the resulting solution was cooled in an ice bath, and the pH was adjusted to 3−4 with dropwise addition of 3 N HCl. This suspension was left at 5 °C for 24 h. The precipitated solid was collected by filtration, washed with brine, and dried in vacuo to afford **2** (0.31 g, 94%) of as an off-white solid: mp 202−204 °C; R_f = 0.35 (MeOH/$CHCl_3$, 1:4); 6.61 (s, 1 H), 7.02 (d, 2 H, J = 8.0 Hz), 7.69 (d, 2 H, J = 8.0 Hz), 8.61 (d, 1 H, J = 7.6 Hz), 10.79 (br s, 1 H). Anal. ($C_{20}H_{20}N_4O_6S_2\cdot 0.31CH_3COCH_3\cdot 0.79HCl$) C, H, N, S.

Construction and Expression of Mutant Human DHFR. Mutations were introduced into the cDNA of human DHFR and verified by sequencing (Roswell Park Cancer Center, Buffalo, NY). DNA oligonucleotides were obtained from Integrated DNA Technologies (Coralville, IA) and used without further purification.

Mutants in pDS5. Plasmid DNA was purified using the plasmid mini kit (Qiagen). Mutagenesis was performed using the QuikChange site-directed mutagenesis kit (Stratagene). All primers were PAGE purified and were synthesized by Alpha DNA (Montreal, Quebec) or IDT (Coralville, IA). Primers were designed according to manufacturer's recommendations. PCR reactions were performed according to manufacturer's recommendations with adjustments made for T_m of corresponding primers. Primers (5′ to 3′) are as follows:

N65F for: GGTTCTCCATTCCTGAGAAGTTTCGACCTTTAAAGGGTAG

N65F rev: CTACCCTTTAAAGGTCGAAACTTCTCAGGAATGGAGAACC

N65S for: GGTTCTCCATTCCTGAGAAGAGTCGACCTTTAAAGGGTAG

N65S rev: CTACCCTTTAAAGGTCGACTCTTCTCAGGAATGGAGAACC

Q36K for: CAGATATTTCAAGAGAATGACCACAACC

Q36K rev: GGTTGTGGTCATTCTCTTGAAATATCTG

Q36S for: CAGATATTTCTCGAGAATGACCACAACC

Q36S rev: GGTTGTGGTCATTCTCGAGAAATATCTG

The original wild type human DHFR (pDS5 vector) was used for PCR and all subsequent mutagenesis experiments. Four single mutants were created (N65F, N65S, Q36K, Q36S) with the QuikChange site directed mutagenesis kit following the manufacturer's recommended conditions: PCR, 50 ng of dsDNA template, 100 ng of each primer, 5 mM dNTPs, 2.5U/μL Taq); one cycle of 95 °C for 30 s; 16 cycles of 95 °C for 30 s, 55 °C for 1 min, 68 °C for 3 min.

The two double mutants (Q35K/N64F and Q35S/N64S) were created by using parental template DNA having one confirmed single residue mutation and using primers for the second desired mutation during PCR.

Expression and Purification of Human DHFR pDS5/Mutant pDS5. Expression of mutant human DHFR in pDS5 vector in *E. coli* BL21 (DE3) was carried out with 200 mL of LB medium containing 100 μg/mL ampicillin and inoculated with glycerol stock of human DHFR at 37 °C with shaking at 300 rpm overnight. Then 1 L of fresh LB/AMP was inoculated with the 200 mL overnight culture. The culture was grown at 37 °C at 300 rpm until the OD_{600} was 0.8−0.9. Cells were then induced with 2 mM IPTG overnight at 16 °C (16−18 h) and harvested by centrifugation at 13000*g*. Cells were resuspended in 100 mL of ice-cold M9 salt solution (12.8 g of $Na_2HPO_4 \cdot 7H_20$, 3 g of KH_2PO_4, 0.5 g of NaCl, 1 g of NH_4Cl in a volume of 1 L).

Cells were lysed in 100 mL of ice-cold buffer containing 6.8 g of KH_2PO_4, 3.7 g of KCl, dissolved in 900 mL of H_20. Then 1.0 mL of 1.0 M EDTA was added and the pH adjusted to 7.0 with KOH before bringing the volume to 1 L. Cells were disrupted by passing through a microfluidizer at 18 000 psi (Microfluidics, Inc.). The resulting lysate was subjected to centrifugation for 30 min at 7000*g*. Ammonium sulfate was added to supernatant over a period of 60 min to a final saturation of 85% at 0 °C. Precipitated protein was centrifuged for 30 min at 7000*g* and the pellet resuspended in 50 mL of methotrexate column binding buffer (100 mM KCl, 50 mM KPO_4, pH 7.0). The resulting sample was passed over a 25 mL methotrexate affinity column. The column was extensively washed (>5 column volumes of buffer) to remove unbound protein. DHFR was subsequently eluted in 5 mL fractions by passing a solution of 4 mM folic acid, 50 mM KPO_4, pH 8.0, over the column. SDS−PAGE was performed on fractions to determine which contained DHFR. The corresponding fractions were then pooled and dialyzed extensively against DEAE column buffer (50 mM KPO_4, pH 7.5) to remove folic acid from solution. On the following day the sample was applied to a 120 mL DEAE ion exchange column (GE Healthcare). The unbound protein fractions (containing DHFR) were collected. Remaining bound proteins and residual folic acid were eluted from the column by a linear gradient of DEAE affinity buffer supplemented with 500 mM NaCl. The column was stripped and regenerated with 1 column volume of 3 M NaCl. All fractions were analyzed by SDS−PAGE. Fractions containing highly pure (>95%) DHFR were pooled, concentrated to 1 mg/mL, flash-frozen in liquid nitrogen, and stored at −80 °C.

Structure Determination and Refinement. The recombinant proteins were washed in a Centricon-10 with 10 mM HEPES buffer, pH 7.4, and concentrated to 33.2 mg/mL. The protein was incubated with NADPH and an excess of the inhibitor for 1 h over ice prior to crystallization using the hanging drop vapor diffusion method. The reservoir solution contained 100 mM KPO_4, pH 6.9, 60% saturated NH_4SO_4, 3% v/v ethanol. Protein droplets contained 100 mM KPO_4, pH 6.9, and 30% saturated NH_4SO_4. Crystals of both mutant and wild type DHFR complexes grew over several days at 14 °C and are trigonal, space group H_3, and diffracted to 1.3 Å resolution. Data were collected at liquid N_2 temperatures on an Rigaku RaxisIV imaging plate system and then later on beamlines 11-1 and 9-2 at the Stanford Synchrotron Research Laboratory (SSRL) imaging plate system. The data were processed with using Mosflm.[41] The R_{merge} for all data was 0.063 with a 3-fold multiplicity. The overall completeness of the data was 94.8 and 92.8 for data in the shell between 2.05 and 2.15 Å. The data for the ternary complex were refined to 17.9% for all data and 25.9% for the test data (5%) (Table 3).

The structures were solved by molecular replacement methods using the coordinates for human DHFR (u072) in the program Molref.[41] Inspection of the resulting difference electron density maps made using the program COOT[42] running on a Mac G5 workstation revealed density for a ternary complex. The final cycles of refinement were carried out using the program Refmac5 in the CCP4 suite of programs. The Ramachandran conformational parameters from the last cycle of refinement generated by PROCHECK[43] showed that more than 97% of the residues have the most favored conformation and none are in the disallowed regions. Coordinates for these structures have been deposited with the Protein Data Bank.

Acknowledgment. This work was supported in part by a grant from the National Institutes of Health and National Institute of Allergy and Infectious Diseases (Grant AI069966 to A.G.) and the National Institute of General Medical Sciences (Grant GM51670 to V.C).

Supporting Information Available: Results from elemental analysis and high resolution mass spectrometry. This material is available free of charge via the Internet at http://pubs.acs.org.

References

(1) Chan, D. C. M; Anderson, A. C. Towards Species-Specific Antifolates. *Curr. Med. Chem.* **2006**, *13*, 377–398.
(2) Hawser, S.; Lociuro, S.; Islam, K. Dihydrofolate Reductase Inhibitors as Antibacterial Agents. *Biochem. Pharmacol.* **2006**, *71*, 941–948.
(3) Gmeiner, H. W. Novel Chemical Strategies for Thymidylate Synthase Inhibition. *Curr. Med. Chem.* **2005**, *12*, 191–202.
(4) Gangjee, A.; Kurup, S.; Namjoshi, O. Dihydrofolate Reductase as a Target for Chemotherapy in Parasites. *Curr. Pharm. Des.* **2007**, *13*, 609–639.
(5) Berman, E. M.; Werbel, L. M. The Renewed Potential for Folate Antagonists in Contemporary Cancer Chemotherapy. *J. Med. Chem.* **1991**, *34*, 479–485.
(6) Blakley, R. L. Dihydrofolate Reductase. In Folate and Pterins; Blakley, R. L., Benkovic, S. J., Eds.; Wiley-Interscience: New York, 1984; Vol. I, pp 191−253.
(7) MacKenzie, R. E. Biogenesis and Interconversion of Substituted Tetrahydrofolates. In Folates and Pterins Chemistry and Biochemistry; Blakley, R. L., Benkovic, S. J., Eds.; Wiley: New York, 1984; Vol. I, pp 255−306.
(8) Petero, G. J.; Kohne, C. H. Fluoropyrimidines as Antifolate Drugs. *Antifolate Drugs Cancer Ther*. **1999**, 101–145.
(9) Rosowsky, A. Chemistry and Biological Activity of Antifolates. In Progress in Medicinal Chemistry; Ellis, G. P., West, G. B., Eds.; Elsevier Science Publishers: Amsterdam, 1989; pp 1−252.
(10) Gangjee, A.; Elzein, E.; Kothare, M.; Vasudevan, A. Classical and Nonclassical Antifolates as Potential Antitumor, Antipneumocystis and Antitoxoplasma Agents. *Curr. Pharm. Des.* **1996**, *2*, 263–280.
(11) Taylor, E. C.; Kuhnt, D.; Shih, C.; Rinzel, S. M.; Grindey, G. B.; Barredo, J.; Jannatipour, M.; Moran, R. A Dideazatetrahydrofolate Analogue Lacking a Chiral Center at C-6, *N*-[4-[2-(2-Amino-3,4-dihydro-4-oxo-7*H*-pyrrolo[2,3-*d*]pyrimidin-5-yl)ethylbenzoyl]-L-glutamic Acid, Is an Inhibitor of Thymidylate Synthase. *J. Med. Chem.* **1992**, *35*, 4450–4454.
(12) Jackman, A. L.; Taylor, G. A.; Gibson, W.; Kimbell, R.; Brown, M.; Calvert, A. H.; Judson, I. R.; Hughes, L. R. ICI D1694, a Quinazoline Antifolate Thymidylate Synthase Inhibitor That Is a Potent Inhibitor of L1210 Tumour Cell Growth in Vitro and in Vivo: A New Agent for Clinical Study. *Cancer Res.* **1991**, *51*, 5579–5586.
(13) Bertino, J. R.; Kamen, B.; Romanini, A. Folate Antagonists. In Cancer Medicine; Holland, J. F., Frei, E., Bast, R. C., Kufe, D. W., Morton, D. L., Weichselbaum, R. R., Eds.; Williams and Wilkins: Baltimore, MD, 1997; Vol. 1, pp 907−921.
(14) Gibson, W.; Bisset, G. M. F.; Marsham, P. R.; Kelland, L. R.; Judson, I. R.; Jackman, A. L. The Measurement of Polyglutamate Metabolites of the Thymidylate Synthase Inhibitor, ICI D1694, in

Mouse and Human Cultured Cells. *Biochem. Pharmacol*. **1993**, *45*, 863–869.
(15) Sikora, E.; Jackman, A. L.; Newell, D. F.; Calvert, A. H. Formation and Retention and Biological Activity of N10-Propargyl-5,8-dideazafolic Acid (CB3717) Polyglutamates in L1210 Cells in Vitro. *Biochem. Pharmacol*. **1988**, *37*, 4047–4054.
(16) Jackman, A. L.; Newell, D. R.; Gibson, W.; Jodrell, D. I.; Taylor, G. A.; Bishop, J. A.; Hughes, L. R.; Calvert, A. H. The Biochemical Pharmacology of the Thymidylate Synthase Inhibitor 2-Desamino-2-methyl-N10-propargyl-5,8-dideazafolic Acid (IC1 198583). *Biochem. Pharmacol*. **1991**, *41*, 1885–1895.
(17) Nair, M. G.; Abraham, A.; McGuire, J. J.; Kisliuk, R. L.; Galivan, J. Polyglutamylation as a Determinant of Cytotoxicity of Classical Folate Analogue Inhibitors of Thymidylate Synthase and Glycinamide Ribonucleotide Formyltransferase. *Cell. Pharmacol*. **1994**, *1*, 245–249.
(18) Gangjee, A.; Qiu, Y.; Li, W.; Kisliuk, R. L. Potent Dual Thymidylate Synthase and Dihydrofolate Reductase Inhibitors: Classical and Nonclassical 2-Amino-4-oxo-5-arylthio-substituted-6-methylthieno[2,3-*d*]pyrimidine Antifolates. *J. Med. Chem*. **2008**, *51*, 5789–5797.
(19) We thank the Developmental Therapeutics Program of the National Cancer Institute for performing the in vitro anticancer evaluation.
(20) Tripos Inc., 1699 South Hanley Road, Suite 303, St. Louis, MO 63144.
(21) Assaraf, Y. G. Molecular Basis of Antifolate Resistance. *Cancer Metastasis Rev*. **2007**, *26*, 153–181.
(22) Matherly, L. H.; Hou, Z. Structure and Function of the Reduced Folate Carrier a Paradigm of a Major Facilitator Superfamily Mammalian Nutrient Transporter. *Vitam. Horm*. **2008**, *79*, 145–184.
(23) Cao, W.; Matherly, L. H. Structural Determinants of Folate and Antifolate Membrane Transport by the Reduced Folate Carrier. In Drug Metabolism and Transport; Lash, L. H., Ed.; Humana Press: Totowa, NJ, 2005; pp 291−318.
(24) Fry, D. W.; Jackson, R. C. Membrane Transport Alterations as a Mechanism of Resistance to Anticancer Agents. *Cancer Surv*. **1986**, *5*, 47–49.
(25) Schornagel, J. H.; Pinard, M. F.; Westerhof, G. R.; Kathmann, I.; Molthoff, C. F. M.; Jolivet, J.; Jansen, G. Functional Aspects of Membrane Folate Receptors Expressed in Human Breast Cancer Lines with Inherent and Acquired Transport-Related Resistance to Methotrexate. *Proc. Am. Assoc. Cancer Res*. **1994**, *35*, 302.
(26) Wong, S. C.; Zhang, L.; Witt, T. L.; Proefke, S. A.; Bhushan, A.; Matherly, L. H. Impaired Membrane Transport in Methotrexate-Resistant CCRF-CEM Cells Involves Early Translation Termination and Increased Turnover of a Mutant Reduced Folate Carrier. *J. Biol. Chem*. **1999**, *274*, 10388–10394.
(27) Webber, S. E.; Bleckman, T. M.; Attard, J.; Deal, J. G.; Katherdekar, V.; Welsh, K. M.; Webber, S.; Janson, C. A.; Matthews, D. A.; Smith, W. W.; Freer, S. T.; Jordan, S. R.; Bacquet, R. J.; Howland, E. F.; Booth, C. J. L.; Ward, R. W.; Hermann, S. M.; White, J.; Morse, C. A.; Hilliard, J. A.; Bartlett, C. A. Design of Thymidylate Synthase Inhibitors Using Protein Crystal Structures: The Synthesis and Biological Evaluation of a Novel Class of 5-Substituted Quinazolines. *J. Med. Chem*. **1993**, *36*, 733–746.
(28) Hughes, A.; Calvert, A. H. Preclinical and Clinical Studies with the Novel Thymidylate Synthase Inhibitor Nolatrexed Dihydrochloride (Thymitaq, AG337). In Antifolate Drugs in Cancer Therapy; Jackman, A. L., Ed.; Humana Press: Totowa, NJ, 1999; pp 229−241.
(29) Gangjee, A.; Guo, X.; Queener, S. F.; Cody, V.; Galitsky, N.; Luft, J. R.; Pangborn, W. Selective *Pneumocystis carinii* Dihydrofolate Reductase Inhibitors: Design, Synthesis, and Biological Evaluation of New 2,4-Diamino-5-substituted-furo[2,3-*d*]pyrimidines. *J. Med. Chem*. **1998**, *41*, 1263–1271.
(30) Gangjee, A.; Jain, H. D.; Kurup, S. Recent Advances in Classical and Non-classical Antifolates as Antitumor and Antiopportunistic Infection Agents: Part II. *Anticancer Agents Med. Chem*. **2008**, *8*, 205–231.
(31) Kovacs, J. A.; Hiemenz, J. W.; Macher, A. M.; Stover, D.; Murray, H. W.; Shelhamer, J.; Lane, H. C.; Urmacher, U.; Honig, C.; Longo, D. L.; Parker, M. M.; Nataneon, J. E.; Parrillo, J. E.; Fauci, A. S.; Pizzo, P. A.; Maeur, H. *Pneumocystis carinii* pneumonia: A Comparison between Patients with the Acquired Immunodeficiency Syndrome and Patients with Other Immunodeficiencies. *Ann. Intern. Med*. **1984**, *100*, 68–71.
(32) Klepser, M. E.; Klepser, T. B. Drug Treatment of HIV-Related Opportunistic Infections. *Drugs* **1997**, *53*, 40–73.
(33) Gewald, K. Heterocyclen aus CH-Aciden Nitrilen. VII. 2-Aminothiophene aus α-Oxo-mercaptanen und Methylenaktiven Nitrilen. *Chem. Ber*. **1966**, *98*, 3571–3577.
(34) Gangjee, A.; Qiu, Y.; Kisliuk, R. L. Synthesis of Classical and Nonclassical 2-Amino-4-oxo-6-benzyl-thieno[2,3-*d*]pyrimidines as Potential Thymidylate Synthase Inhibitors. *J. Heterocycl. Chem*. **2004**, *41*, 941–946.
(35) Taylor, E. C.; Young, W. B.; Chaudhari, R.; Patel, M. Synthesis of a Regioisomer of *N*-{4-[2-(2-amino-4(3*H*)-oxo-7*H*-pyrrolo[2,3-*d*]pyrimidin-5-yl)ethyl]benzoyl}-L-glutamic Acid (LY231514), an Active Thymidylate Synthase Inhibitor and Antitumor Agent. *Heterocycles* **1993**, *36*, 1897–1908.
(36) Itoh, T.; Mase, T. A General Palladium-Catalyzed Coupling of Aryl Bromides/Triflates and Thiols. *Org. Lett*. **2004**, *24*, 4587–4590.
(37) Gangjee, A.; Yu, J.; McGuire, J. J.; Cody, V.; Galitsky, N.; Kisliuk, R. L.; Queener, S. F. Design, Synthesis, and X-ray Crystal Structure of a Potent Dual Inhibitor of Thymidylate Synthase and Dihyhdrofolate Reductase as an Antitumor Agent. *J. Med. Chem*. **2000**, *43*, 3837–3851.
(38) Cody, V.; Galitsky, N.; Luft, J. R.; Pangborn, W.; Gangjee, A.; Devraj, R.; Queener, S. F.; Blakely, R. L. Comparison of Ternary Complexes of *Pneumocystis carinii* and Wild Type Human Dihydrofolate Reductase with a Novel Classical Antitumor Furo[2,3-*d*]pyrimidine Antifolate. *Acta Crystallogr*. **1997**, *D53*, 638–649.
(39) Kisliuk, R. L.; Strumpf, D.; Gaumont, Y.; Leary, R. P.; Plante, L. Diastereoisomers of 5,10-Methylene-5,6,7,8-tetrahydropteroyl-D-glutamic Acid. *J. Med. Chem*. **1977**, *20*, 1531–1533.
(40) Wahba, A. J.; Friedkin, M. The Enzymatic Synthesis of Thymidylate. Early Steps in the Purification of Thymidylate Synthetase of *Escherichia coli*. *J. Biol. Chem*. **1962**, *237*, 3794–3801.
(41) Collaborative Computational Project, Number 4. The CCP4 suite: programs for protein crystallography. *Acta Crystallogr*. **1994**, *D50*, 760−763.
(42) Emsley, P.; Cowtan, K. Coot: Model-Building Tools for Molecular Graphics. *Acta Crystallogr*. **2004**, *D60*, 2126–2132.
(43) Laskowski, R. A.; MacArthur, M. W.; Moss, D. S.; Thornton, J. M. PROCHECK: A Program To Check the Stereochemical Quality of Protein Structures. *J. Appl. Crystallogr*. **1993**, *26*, 283–291.